

Structural, dielectric and optical investigation of chemically synthesized Ag-doped ZnO nanoparticles composites

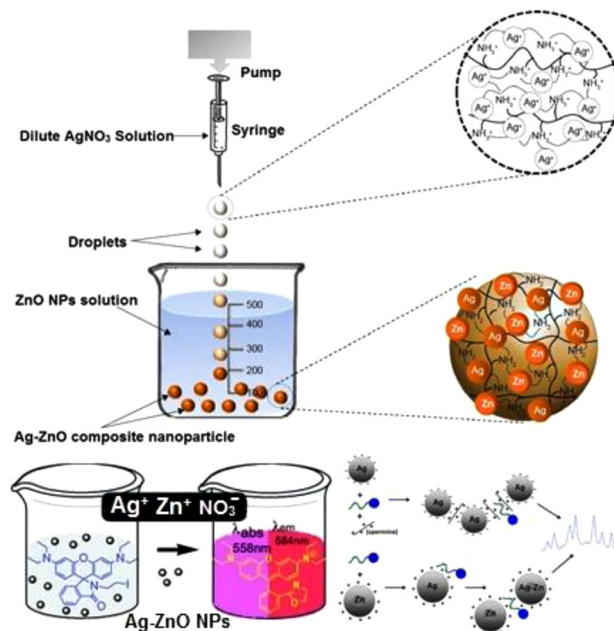
Suresh Sagadevan¹ · Kaushik Pal² · Zaira Zaman Chowdhury³ · M. Enamul Hoque⁴

Received: 21 March 2017 / Accepted: 11 May 2017 / Published online: 20 May 2017
© Springer Science+Business Media New York 2017

Abstract The sol–gel technique was used in the chemical synthesis and characterizations based on structural, morphological, optical and electrical studies of pure and Ag-doped zinc oxide (ZnO) nanoparticles. X-ray diffraction, scanning electron microscopy, energy Dispersive X-ray spectrometry, transmission electron microscope, ultraviolet spectroscopy, photoluminescence and FT-IR analysis were used to perform the characterization of the morphological analysis, optical studies, phase purity and crystalline size. The Powder X-ray diffraction results proved polycrystalline nature of ZnO with a hexagonal wurtzite structure. Debye-Scherrer's formula was used to evaluate the average crystallite size of pure and Ag-doped ZnO. Their values have been determined to be 14 and 18 nm respectively. To examine the various functional groups FTIR was utilized. The unique aggregation of the particles was stated by the scanning electron microscopy investigation and transmission electron microscope analysis was used to substantiate the nanosphere formation. Here, the estimated optical band gap value for pure and Ag-doped ZnO nanoparticles was 3.22 and 3.17 eV, respectively. UV–visible spectroscopy was used to perform this process. Photoluminescence

studies have proved the Ag-doped ZnO sample of the blue shift emission bands. At different frequencies and temperatures, under specific conditions, the dielectric properties like dielectric constant, dielectric loss and AC conductivity of Ag-doped ZnO nanoparticles were analyzed.

Graphical Abstract



✉ Suresh Sagadevan
drsureshnano@gmail.com

- ¹ Department of Physics, AMET University, Chennai 603 112, India
- ² Engineering & Nanoscience & Building, Wuhan University, 8 East Lake South Road, Wuchang 430072, PR China
- ³ Nanotechnology & Catalysis Research Centre, University of Malaya, Kuala Lumpur 50603, Malaysia
- ⁴ Department of Biomedical Engineering, King Faisal University, Al - Hofuf, Al - Ahsa 31982, Saudi Arabia

Keywords Ag-doped ZnO nanoparticles composite · Sol-gel · Optical and dielectric studies

1 Introduction

The science that involves the study of various structures of matter at the scale of a billionth of a meter is termed as nanotechnology. Besides it includes the change of matter in nanometer scales to produce novel structures and devices. Generally, nano particle's size is estimated to be between 1–100 nm. Nanoparticles possess various physical and chemical properties of bulk metals which comprises low melting point, high specific surface areas, good optical properties, mechanical strength, and specific magnetizations. Thus in electronics, medicine and other areas of Nanotechnology plays a significant role. Presently in electronic industries semiconductors and magnetic materials play an important role. In diluted magnetic semiconductors, new materials can be found by combining the properties of semiconductors and magnetic materials thus enhancing the device performance. When compared to electronics magneto electronics exhibit an important character where the magnet tends to remain magnetized for a longer duration of time. Therefore, it happens to be an immense field of attraction among the researchers to use magnetic material as an alternative to the semiconductor-based components of the computer. Broad studies in photochemistry and environmental protection have been performed for semiconductor photocatalysts, like the photocatalytic degradation of environmental pollutants. Conversely, wide research activities in the transition–metal oxide semiconductor nanomaterials attract considerable attention to their distinctive physical and chemical properties and varied applications in the optical and electronic field [1]. Zinc oxide (ZnO) nanostructures are widely examined amidst different type of metal oxides because of their massive potential for electronic, photonic and spintronics applications. Furthermore, they have an extensive use in the gas sensors, biosensors, and solar cell applications [2].

ZnO is an n type semiconductor which, at room temperature, exhibits a direct band gap of 3.37 eV with an exciton binding energy of 60 meV [3]. Zinc oxide (ZnO) is the II–VI group of semiconductor materials and it is a very promising material for semiconductor device applications [4]. Besides, it is also biocompatible, bio-safe and phototoxic intracellular [5]. At room temperature ZnO doped with transition metal ions, indicate various applications, like the n-type doped nanolaser, p-type doping and room temperature ferromagnetic semiconductor nanomaterials [6]. Generally, nanostructured ZnO is intensively attractive in the improvement of nano generators, solar cells, Light emitting devices, spintronic, varistors, biological sensors, photonic devices, and in data storage devices, thus making it a very noteworthy material [7, 8]. Optical, magnetic, and electrical properties of the ZnO nanoparticles were improved by the addition of dopants. ZnO in visible light, exhibit improved

photo catalytic activity when hybridized with noble metals has been reported [9–11]. Various dopants were used to dope with ZnO samples, modification in the orientation and morphology are performed either by thermal treatment or by concentration variation and dopant types [12–14]. The ZnO has various dopants in Group-Ib among possible acceptor dopants and silver is a good candidate for producing a shallow acceptor level in ZnO [15]. At high temperature it exhibits good stability and compatibility with other transparent conducting oxide materials that makes Ag-doped ZnO appropriate for transparent and optoelectronic related technological applications. To obtain better efficiency of luminescence Ag is preferred [16]. So far, different techniques were used in the manufacture of doped ZnO nanoparticles. These methods may be sol–gel technique soft chemical route, co-precipitation method, hydrothermal method, and solvo-thermal method [3, 17–20]. Here the paper gives details about the Ag-doped ZnO nanoparticles preparation and their structural, surface morphology, optical, and dielectric studies which is also reported. However, the nano sized silver and zinc oxide belongs to the high affinity of antibacterial properties, so Ag-doped ZnO nanocomposites may be utilized in chemical and biological sensors to control the bacterial growth in a variety of applications, including medical devices, dental composite materials, and textile materials. Moreover, the silver (Ag) has been extensively used in topical preparations and to saturate bandages so as to restrict bacterial growth in injured skin. Thus, addition of silver in zinc oxide may result in varied particle size and hence may affect its antibacterial activity. Novelty of work in this article deals with the preparation of Ag-doped ZnO nanoparticles and their electrical properties have been reported.

2 Experimental details

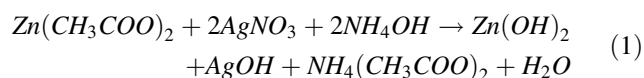
2.1 Preparation of Ag-doped ZnO nanoparticles

All chemical reagents have been commercial with AR purity and are utilized directly without any additional purification. The sol–gel technique was utilized in this experimental work for the pure and Ag-doped ZnO nanoparticles synthesis.

In brief, sol–gel synthesis 0.25 M of zinc acetate [$\text{Zn}(\text{CH}_3\text{COO})_2 \cdot 2\text{H}_2\text{O}$] and 0.002 M silver nitrate (AgNO_3) was mixed with 50 ml of deionized distilled water. A 2.0 ml of 25% ammonia solution (NH_4OH) added drop wise until precipitation occurred and then further 10 drops of ammonia solution (NH_4OH) added to make the transparent solution followed by vigorous stirring, the value of pH of the starting solution was maintained at 9.5. Later, surfactant triethanolamine ($\text{C}_6\text{H}_{15}\text{NO}_3$) was added to control the size

and structural morphology. Hence, the pulse mode sonication (PS) operated at 100 W, the frequency of the sonicator maintained at 30 kHz \pm 50 Hz. PS takes place for one second then stops for one second, and the total process took 3 h to gel precipitation. The initial pH of the solution was 9.5 whereas at the end, the pH was 8.2 and the solution became clear silvery white and gradually gel suspension is settled and then placed into sealed polypropylene containers. The formed gel was washed several times with deionised water and acetone followed by the complete elimination of acetate salt. The final gelation transparent products were obtained grinding bulk powders into fine powder. Indeed, high flow of N₂ air through the fine powders in a vacuum for 20 min. These desired powders were calcined for 2 h at temperature 300 °C in a furnace atmospheric pressure to obtain dry powders.

Ammonia solution (NH₄OH) was used as a precipitating agent during synthesis between zinc acetate [Zn(CH₃COO)₂·2H₂O] and silver nitrate AgNO₃ with water (H₂O) to form Zn(OH)₂, AgOH, NH₄(CH₃COO)₂, NH₄NO₃, and H₂O. The product was washed with deionised water for several times to form Zn(OH)₂, AgOH and H₂O. Then again washed with acetone by centrifuging in order to form Zn(OH)₂ and AgOH. On heating at 300 °C the product obtained was pure ZnO doped Ag₂O like (Zn–O–Ag) in the precursor. Through the sol–gel assisted route and solvothermal treatment, the precursor reduced by acetone gradually and Zn–O ∞ Ag bond formation between Ag-doped ZnO nanocomposite material, which have been explained below;



(Washed with DD H₂O by 3 times)

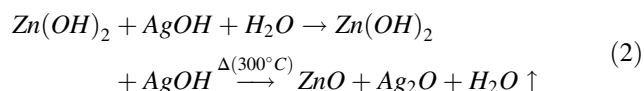


Figure 1 represents a schematic diagram in detailed synthesis method displayed below.

2.2 Characterization techniques and instrumental analysis

The Ag-doped ZnO nanoparticles' crystalline size and structure were analyzed by X-ray diffraction (XRD) method where powder X-ray diffractometer (Schimadzu model: XRD 6000 with CuK α (λ = 0.154 nm) radiation with a diffraction angle between 30° and 80° was used. FTIR model Bruker IFS 66 W Spectrometer was used to attain the FTIR spectrum. Scanning electron microscope (SEM) using JEOL; JSM- 67001 was used to examine the surface morphology of the Ag-doped ZnO nanoparticles. To verify the

size of the synthesized particle transmission electron microscope (TEM) with an H-800 TEM (Hitachi, Japan) and 100 kV as the accelerating voltage was utilized. ELICO SL-159 UV–Visible conventional spectrophotometer at the range of 300–1100 nm evaluated the absorption spectrum. Perkin-Elmer lambda 900 spectrophotometer recorded the photoluminescence (PL) spectrum. Here Xe lamp acted as the excitation light source. At various temperatures the dielectric constant and dielectric loss of the pellets of Ag-doped ZnO nanoparticles in disk form were investigated. This was done by the HIOKI 3532-50 LCR HITESTER at a frequency range of 50 Hz to 5 MHz. Samples were obtained having a diameter of ~12 mm and thickness of ~1 mm for evaluation. With a conventional four terminal specimen holder the specimen was situated amidst the electrodes for examination. This includes temperature variations besides a conventional two terminal sample of the surrounding conditions. Between the copper platforms and electrodes the sample was mounted. Silver paint was used to coat the faces to ensure immense electrical contact. The capacitance and dissipation factor of the parallel plate capacitor shaped by the copper plate and the terminal having the specimen as a dielectric medium was measured.

3 Results and discussion

3.1 Structural analysis

Figure 2 presents the X-ray diffraction pattern of the pure and Ag-doped ZnO nanoparticles. The diffraction peaks corresponding to (1 0 0), (0 0 2), (1 0 1), (1 0 2), (1 1 0), (1 0 3), (1 1 2), and (2 0 1) planes were found. The hexagonal wurtzite structure of ZnO is substantiated by the planes confirming the high purity nature of the synthesized powder [21]. The diffraction peaks related to impurities were not obtained from the XRD pattern. Moreover, the intensity diffraction peaks are broadening and it reduces as the Ag content increases, which occurs by the substitution of Ag ions with the ZnO host lattice size. Scherrer's formula [22] was used in verifying the average grain size of the Ag-doped ZnO nanoparticles from the prominent peak in the XRD,

$$D = \frac{0.9\lambda}{\beta \cos \theta} \quad (3)$$

where λ is the X-ray wavelength, θ is the Bragg diffraction angle and β is the full width at half maximum of the XRD peak occurring at the diffraction angle of θ . The average grain size of pure and Ag-doped ZnO nanoparticles was evaluated to be 14 and 18 nm, respectively.

Fig. 1 Schematic representation of Ag-doped ZnO nanoparticles composite by ion exchange via sol-gel chemical route

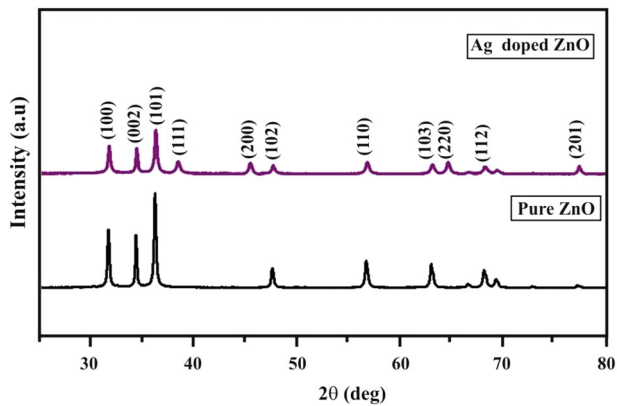
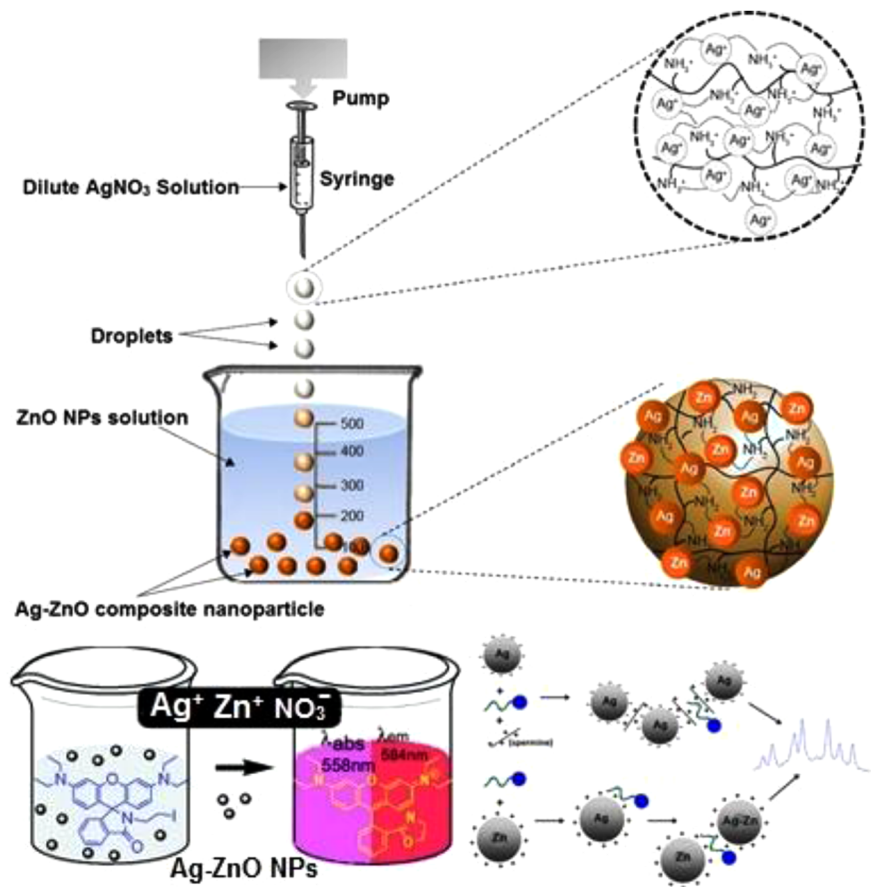


Fig. 2 XRD pattern of pure and Ag-doped ZnO nanoparticles

3.2 FTIR analysis

To study the functional groups or the chemical bond types, FTIR is used. Figure 3 shows the FTIR spectra of pure and Ag-doped ZnO nanoparticles. Because of the stretching mode of an O–H group, a broad absorption band at 3428 cm^{-1} occurs proving the presence of a small amount of water that was absorbed by the ZnO nanostructure [23]. The vibration of 1608 cm^{-1} is attributed to the tinhydroxyl (Zn–OH) bond. The band that occurred between 400 and

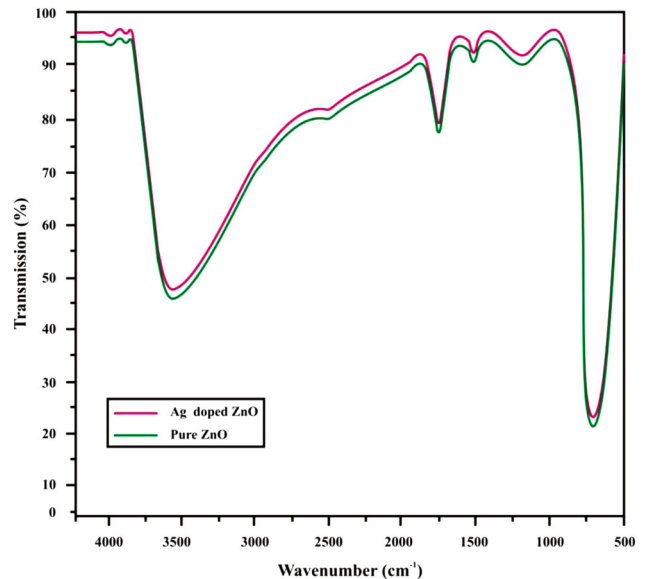


Fig. 3 FTIR spectrum of pure and Ag-doped ZnO nanoparticles

750 cm^{-1} is correlated with the metal oxide bond (ZnO) [24, 25]. At the peak a minor shift was found in the Ag-doped ZnO. Change in the band position towards the low frequency can be associated with the bond length changes

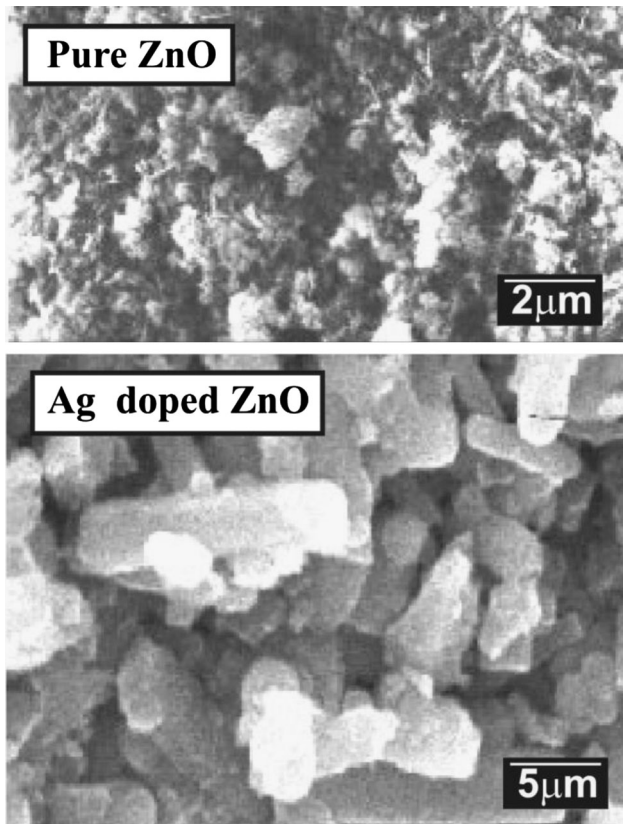


Fig. 4 SEM image of Ag-doped ZnO nanoparticles

because of the partial substitution of Ag^+ ion at the ZnO lattice site [26].

3.3 Surface analyses by SEM and EDX

Typical SEM images signifies the pure and Ag-doped ZnO nanoparticles composite are shown in Fig. 4. The microstructure formed exhibited uniform and compact structure, interconnected by grains. The result shows large grain size. Figure 5 shows the qualitative elemental analysis results performed using energy dispersive X-ray (EDX) analysis for Ag-doped ZnO nanoparticles. Clear peaks were shown by the EDX spectrum corresponding to Ag, Zn and O.

3.4 Microstructure analysis

TEM is usually helpful in imaging and analytical characterization of the nanoparticles and to evaluate the shape, size and morphology. A typical TEM image of Ag-doped ZnO nanoparticles is shown in Fig. 6a. The particles that are almost similar and uniform particles size of 20 to 35 nm, were shown in this image. Hence, Ag-ZnO nanoparticle composite was confirmed in Fig. 6b. While the selected area diffraction (SAED) pattern of the nanocomposites information can be illustrated in Fig. 6c. The detail

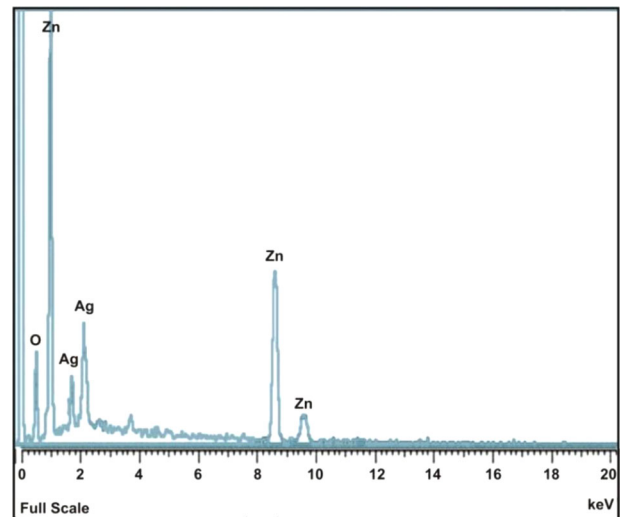


Fig. 5 EDX spectrum of Ag-doped ZnO nanoparticles

investigations of SAED patterns of ‘red’ outlined with an arrow explores polycrystalline in nature of Ag-ZnO nanocomposite materials of Ag and Zn same lattice plane [1 0 1], but different orientation indicated by ‘white’ arrow as depicted in Fig. 6d, the circular white patches are exhibited in the field of view exhibits the nanocrystalline particles [27].

3.5 Optical studies

Optical absorption of high energy lights by atoms or molecules. UV–visible spectroscopy was utilized which led to electronic excitation. To characterize the optical properties of pure and Ag-doped ZnO nanoparticles, UV–vis. absorption spectroscopy was utilized. Figure 7 presents the absorption spectrum of pure and Ag-doped ZnO nanocomposites. In Ag-doped ZnO samples the absorption edge shifted towards the higher wavelength side (red shift) and also the intensity was increased. The changes in the absorption peaks, due to doping, showed changes in the band structure and decreasing the band gap energy of pure ZnO. This occurs by the quantum confinement of the photo generated electron–hole pairs. From transmittance, the optical absorption coefficient (α) was evaluated by [11];

$$\alpha = \frac{1}{d} \log \left(\frac{1}{T} \right) \quad (4)$$

where T is the transmittance and d is the thickness. For high photon energies ($h\nu$) the absorption coefficient (α) obeys the relation [12];

$$\alpha = \frac{A(h\nu - E_g)^{1/2}}{h\nu} \quad (5)$$

where α , E_g and A are the absorption coefficient, band gap and constant respectively. In the Fig. 8 shows a plot of

Fig. 6 **a** TEM image of pure ZnO-NPs, **b** Ag-doped ZnO nanoparticle composites, **c** selected area diffraction (SAED) pattern, and **d** polycrystalline lattice plane at different orientation of nanocomposites

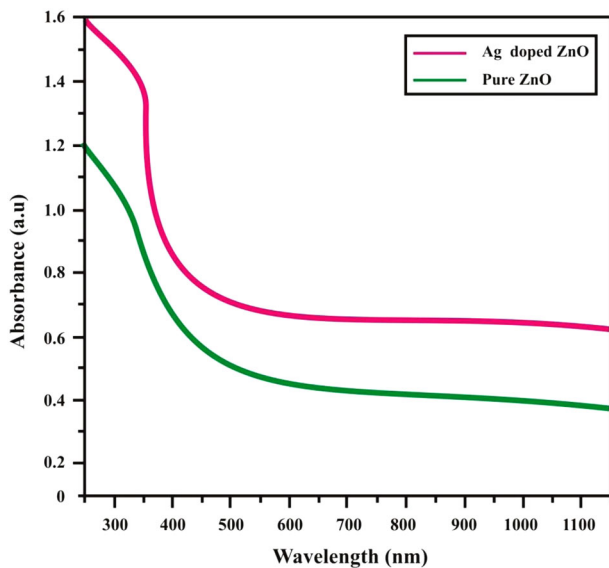
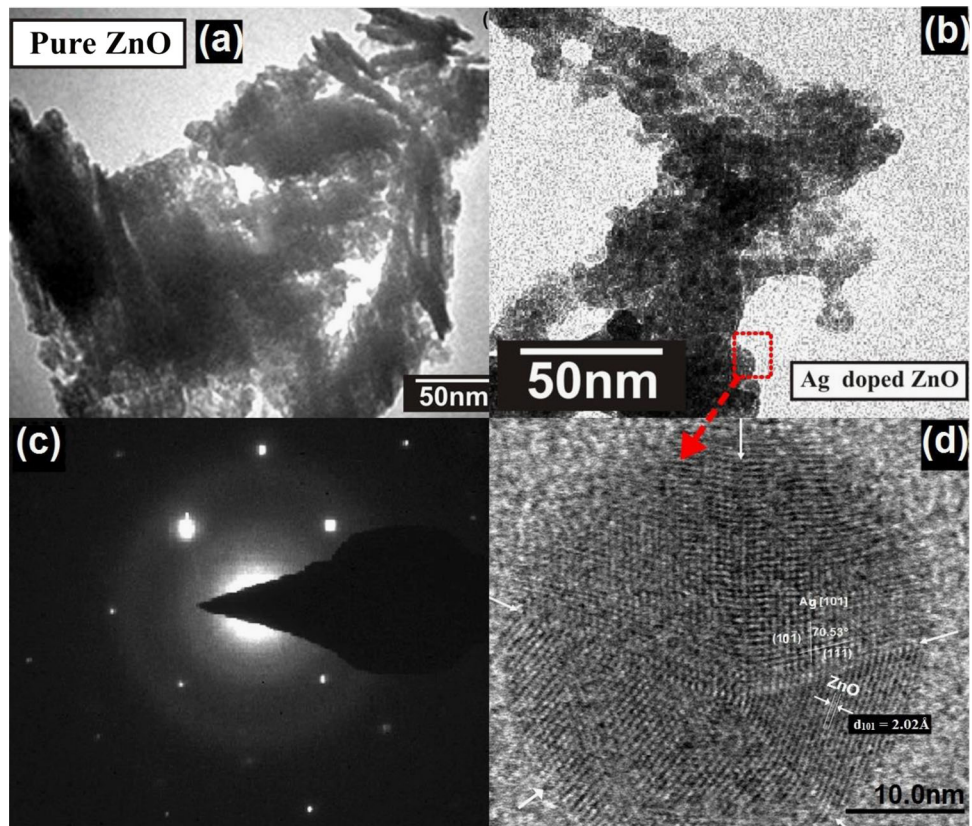


Fig. 7 UV-visible absorption spectrum of pure and Ag-doped ZnO nanoparticles

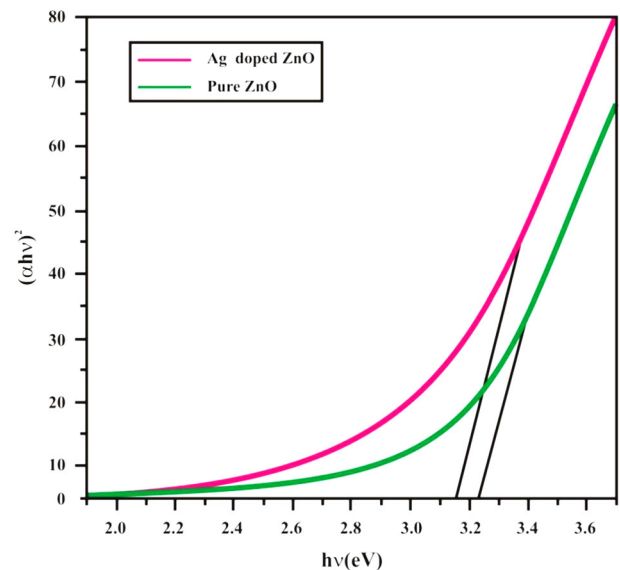


Fig. 8 Evaluation of $[(ah\nu)^2]$ plotted against photon energy ($h\nu$) for the optical energy band (E_g) diagram of pure and Ag-doped ZnO nanoparticles

$(ah\nu)^2$ against $h\nu$. By extrapolating the rising part of the absorption peak, the band gap of the prepared samples was estimated. The evaluated band gap values for pure and Ag-doped ZnO nanoparticles were determined to be 3.22 and 3.17 eV respectively. When Ag atoms are doped with ZnO, the zinc sites get occupied by the Ag atoms in the ZnO

lattice thus reducing the band gap of ZnO doped with the acceptor [28]. Reducing the band gap occurs with the presence of p-type conductivity in the ZnO nanoparticles doped with Ag. Ag doping in ZnO provides impurity band in the energy gap. This occurs by the formation of p-type

within the substance. Such widening of band gap is referred as blue-shift [29].

3.6 PL spectrum analysis

A common tool used to probe the electron–hole surface processes of semiconductor, estimating of band-gap energy and surface defect within the sample materials is the PL. Figure 9 presents the PL emission spectra of both pure and Ag-doped ZnO nanoparticles. The PL peak is observed at 392 nm for the ZnO nanoparticles. Whereas the Ag-doped ZnO peak observed to be in the 398 nm range. The emission peaks 392 nm is attributed to characteristic emission of ZnO and arises from the band-edge transition or exciton recombination. This result clearly states a shift in the PL peak in the higher photon energy region to lower region of photon energy. There occurs a change that shifts slightly towards the side of higher wavelength. The first emission occurs because of recombination of holes and electrons that are present at the valence and conduction bands. Occurrence of blue shifts in UV region is indicated in this observation. This occurs because of the displacement of Fermi level towards the conduction band in the ZnO material which further leads to band gap widening. Ag incorporation is apparently exploring the competitive phenomenon of blue–green (450–560 nm) PL emission [30]. The blue–green emission peak at 492 nm is due to electron transmission, mediated by defect levels in the band gap, such as oxygen vacancies, zinc interstitials and so forth. Origination of this behavior is because of the favorable transmission between the localized states that are produced

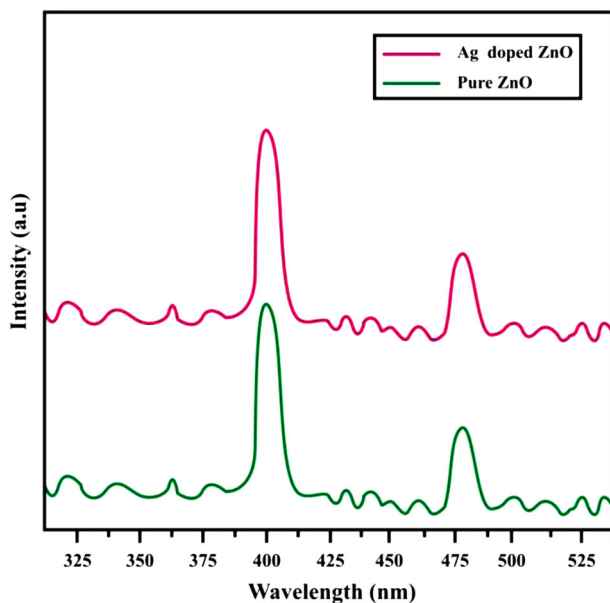


Fig. 9 Photoluminescence spectra of Ag-doped ZnO nanoparticles

by the Ag-dopant or owing to the reduction in the self-activated centers by the presence of Ag^+ ions in the Zn vacancies [31]. All peak intensity was made higher, thus shifting towards the higher wavelength size. This result proposes the optical property of pure ZnO that was enhanced extensively through Ag doping and also reducing the band gap energy of ZnO nanoparticles.

3.7 Dielectric properties

In disk form, at different temperatures, the pure and Ag-doped ZnO nanoparticle pellets were studied. At different temperatures and at a frequency range between 50 Hz–5 MHz, the dielectric constant and dielectric loss for pure and Ag-doped ZnO nanoparticles were investigated. The dielectric constant was evaluated by using the relation [13];

$$\epsilon_r = \frac{Cd}{\epsilon_0 A} \quad (6)$$

Where, d and A being the thickness and area of the sample respectively. With respect to frequency and temperature, Fig. 10 shows variation in the dielectric constant of pure ZnO nanoparticles. Pure ZnO nanoparticles, at low frequencies, have increased dielectric constant which rapidly reduces with the applied frequency at all temperatures. The high dielectric constant value may be characterized to high ion jump orientation effect and increased space charge effect exhibited by the nanoparticles. Most atoms in the nanocrystalline materials are present at the grain boundaries that, become active electrically because of charge catching. At low frequency values, dipole moment can effortlessly follow the changes in electric field. The contribution towards the increment in dielectric constant occurs because of the space charge and rotation polarization, which takes

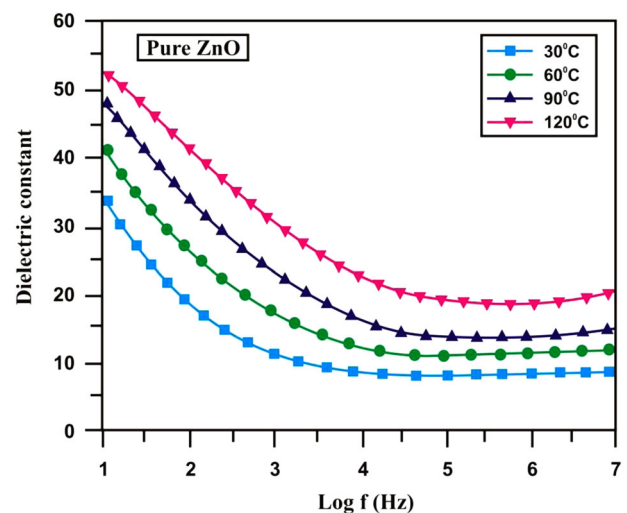


Fig. 10 Dielectric constant of pure ZnO nanoparticles

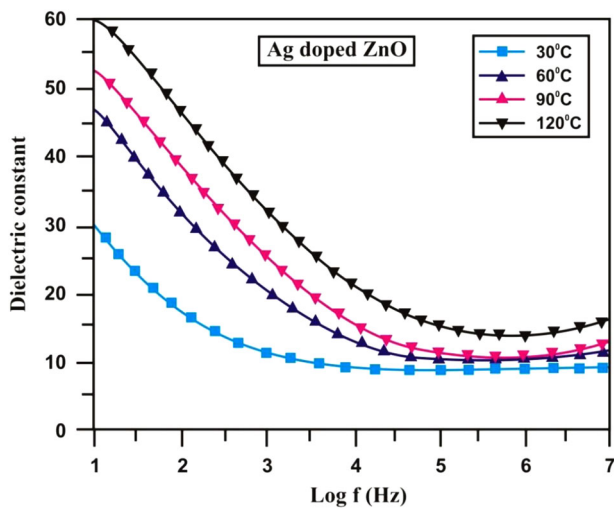


Fig. 11 Dielectric constant of Ag-doped ZnO nanoparticles

place mostly at the interfaces. Thus, the dielectric constant of nanostructures materials should be higher when compared to other conventional materials. The reason for increased dielectric constant of nanocrystalline materials at high temperature of higher space charge polarization owing to the structure of their grain limit interfaces. Similarly, at high temperature, sharp increase of the dielectric constant rules the dielectric loss at lower frequencies and temperatures. As the temperature goes higher, space charge and ion jump polarization decreases, thus leading to a dielectric constant reduction.

For Ag-doped ZnO nanoparticles, the dielectric constant was estimated as a function of frequency at various temperatures is shown in Fig. 11. At lower frequency, the strength of frequency dependence is very clear. As the frequency goes higher the dielectric constant gets decreased, finally attaining a constant value at high frequencies. As the dielectric constant value decreases with increasing frequencies and it can be elucidated on the interface/space charge polarization due to inhomogeneity in the dielectric structure [32]. Porosity and grain structure are the inhomogeneities present in the system. Polarization got decreased as the frequency increases and it attained a constant value. This occurs beyond a certain frequency of external field the hopping between various metal ions could not follow the alternating field. As the dopant concentration increases, there is a presence of high silver ions which leads to the decrease in dielectric polarization, which reduces the dielectric constant. Hence, as the dopant concentration increases more Zinc ions will be substituted by silver ions and thereby decreasing the dielectric polarization, which in turn decreases the dielectric constant.

Figure 12 shows the variation in dielectric loss of pure ZnO with frequency and temperature. It is clear that the dielectric loss decreases with an increase in frequency. The

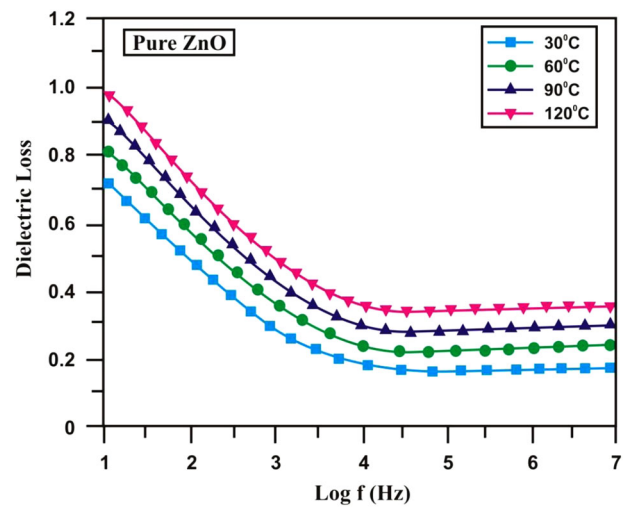


Fig. 12 Dielectric loss of pure ZnO nanoparticles

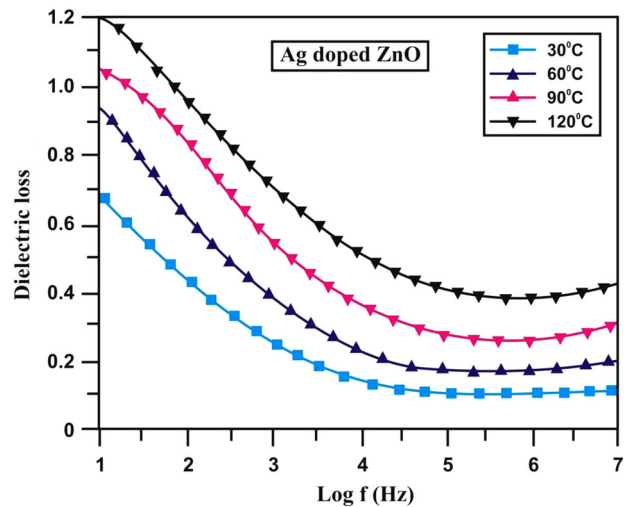


Fig. 13 Dielectric loss of Ag-doped ZnO nanoparticles

loss angle at higher frequencies has almost similar values at all temperatures. In polar dielectrics, the molecular orientation along the direction of applied electric field requires a part of electric energy to surmount the internal friction forces. The revolutions of dipolar molecules and various types of molecular transfer from one position to the next uses up a part of electric energy which led to energy losses. Inhomogeneities related to defects and the space charge arrangement in the inter phase layers form absorption current that results in dielectric loss in the nanophase materials. Figure 13 presents the curve of dielectric loss vs. log f for Ag-doped ZnO nanoparticles at various temperatures. It is found that, at all temperatures, as the frequency increases dielectric loss reduces, which occurs due to the space charge polarization [33]. It is also known that the reduction in occurred as the frequency increases and it got reduced at higher frequency region. It shows the capability of these

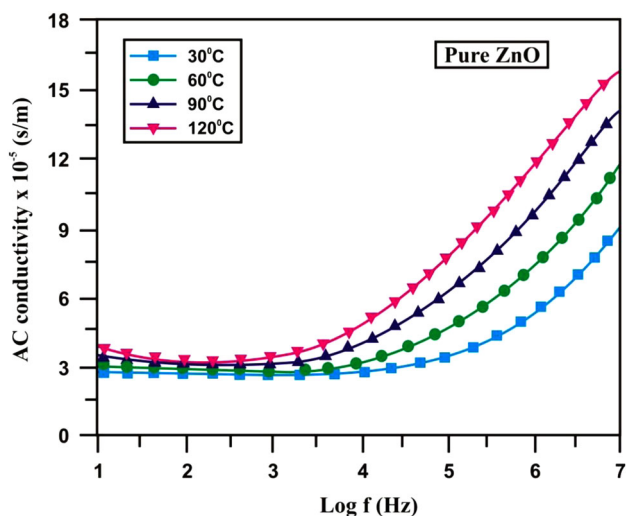


Fig. 14 Variation of AC conductivity of pure ZnO nanoparticles

materials that are used in high frequency device applications [34].

3.8 AC conductivity measurement

The AC conductivity plot for the pellets of pure and Ag-doped ZnO nanoparticles have been investigated. It is found that the AC conductivity progressively increases with the increase in the frequency of the applied AC field. This is because rising in frequency would improve the electron hopping frequency. The AC conductivity of pure and Ag-doped ZnO nanoparticles can be determined using the following relation [35–38];

$$\sigma_{ac} = 2\pi\epsilon_0\epsilon_r f \tan \delta \quad (7)$$

where ϵ_0 is the permittivity of free space, ϵ_r is dielectric constant, f is the frequency and $\tan \delta$ is the loss factor. Figure 14 illustrates the variation in AC conductivity of pure ZnO nanoparticles at various frequencies and temperatures. It is seen that the AC conductivity increases as the frequency increases. It is also clear from the figure that, electrical conductivity increases with the increasing of frequency in the various temperatures. At higher temperature, a higher AC conductivity value has been observed. This is due to the short range translational hopping of charge carriers between the localized states [39]. The AC conductivity plot of pure and Ag-doped ZnO nanoparticles pallets is shown in Fig. 15. The electrical conductivity exhibits minute increase in the nanomaterial at low frequency region for as the frequency increases and it remains the same at all temperatures. Conversely, at high frequency value, particularly in KHz, there occurs a rapid increase in the conductivity value and it becomes enormous at high temperature which can be attributed to little Polaron jumping [40]. At low frequency region, it is found that the

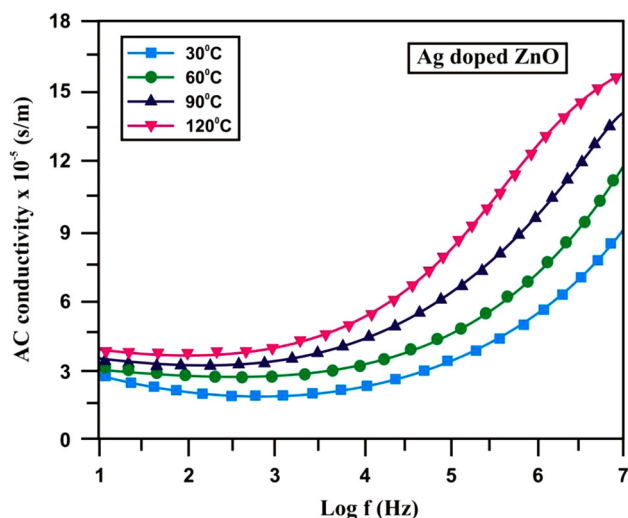


Fig. 15 Variation of AC conductivity of Ag-doped ZnO nanoparticles

frequency independent behavior that characterizes the DC conductivity and dispersion at higher frequency region exhibits the behavior of frequency dependence. It is consistent as the temperature increases resulting in a huge carrier hopping, which causes the conductivity to go higher.

4 Conclusions

In summary, the above presented experimental results and discussions revealed that Ag-doped ZnO nanocomposite materials were synthesized that concise the following conclusions:

1. Sol–gel chemical assisted process is an easy and simple route played an efficient task in the synthesis of Ag:ZnO nanocomposite material when compared with other methods.
2. In the pulse mode (PS) synthesizes, precursor and reducing agent are the main reasons for the morphological changes during sol–gel synthesis.
3. Addition of Ag^+ ions during dispersion (pulse mode) through ultrasonication increases high crystalline nature and the change in crystallographic morphology.
4. Ag^+ ion rests upon the surface of the ZnO at some stage to form truncated nanoparticle morphology.
5. Temperature, time, and alteration of initial and final pH also plays prominent role in forming different size and morphological evolution of Ag-doped zinc oxide nanocomposite (Ag:ZnO).

However, XRD confirmed the formation of Ag-doped ZnO nanoparticles. It was known from the XRD analysis that the acquired hexagonal wurtzite structure of polycrystalline ZnO and the average crystallite size of pure and

Ag-doped ZnO were found to be 14 and 18 nm, respectively. FTIR analysis was used to confirm the various functional groups. The fact that the particles are strongly aggregated was clearly verified by the SEM observation. pure and Ag-doped ZnO nanoparticle absorption took place in the UV region was confirmed by the UV–Vis spectrum. The band gap values for pure and Ag-doped ZnO nanoparticles were evaluated and found to be 3.22 and 3.17 eV respectively. The presence of the blue shift emission band in the Ag-doped ZnO sample was provided by PL studies. Analysis pertaining the variations in dielectric constant, dielectric loss and AC conductivity with frequency and temperature for pure ZnO nanoparticles was performed. Inverse variation, i.e., (decreased) with the frequency, in the dielectric constant and dielectric loss was revealed by the dielectric studies. The AC electrical conductivity was directly proportional to the temperature and frequency. The changes in the dielectric constant, dielectric loss, and AC conductivity were investigated for Ag-doped ZnO nanoparticles. The dielectric studies proved that both the dielectric constant and dielectric loss reduces as the frequency increases. There was a sudden drop in the dielectric constant at lower frequencies. The Ag dopant concentration increased more by reducing the dielectric polarization because of the interface/space polarization, which in turn reduced the dielectric constant. The Ag dopant concentration increased more by reducing the dielectric polarization because of the interface/space polarization, which in turn reduced the dielectric constant. Moreover, the increase of AC electrical conductivity was observed with an increase of temperature and frequency. Finally, it was realized that the several unique features of synthesized Ag:ZnO was observed with the deserved special comments. The generality and simplicity for the synthesis of Ag-doped ZnO nanocomposite materials are involved in complete sol-gel trouble-free steps.

Acknowledgements The authors are grateful to *AMET University and Anna University in Chennai* for essential samples preparation and characterization. Especially, the author Dr. Kaushik Pal, warm wishes and thanks to his associate colleagues & Bachelor/Masters students, instrumental operators who provided a friendly research environment in *Wuhan University, China*.

Compliance with ethical standards

Conflict of interest All the authors declare that they have no competing interests.

References

- Parthibavarman M, Hariharan V, Sekar C, Singh VN (2010) *J Optoelectron Adv Mater* 12:1894–1898
- Parthibavarman M, Jayashree M, Sharmila V (2016) *Int J Multidiscip Res Rev* 1:231–235
- Saravanakumar K, Sakthivel B, Ravichandran K (2011) *Mater Lett* 65:2278–2280
- Pooja D, Sharma SK, Knobel M, Rani R, Singh Res M (2012) *J Recent Sci* 1:48–52
- Arooj S, Nazir A, Nadhman N, Ahmad B, Muhammad I, Ahmad K, Mazhar R (2015) *Beilstein J Nanotechnol* 6:570–582
- Sankara Reddy B, Venkatramana Reddy S, Koteeswara Reddy N, Prabhakara Reddy Y (2014) *Adv Mater Lett* 5:199–205
- Rana SB, Singh P, Sharma AK, Carbonari AW, Dogra R (2010) *J Opto Electron Adv Mater* 12:257–261
- Murugadoss G (2012) *J Mater Sci Technol* 28:587–593
- Caglar M, Yakuphanoglu F (2012) *Appl Surf Sci* 258:3039–3044
- Pal K, Maiti UN, Majumder TP, Debnath SC (2013) *J Mol Struct* 1035:76–82
- Pal K, Majumder TP, Debnath SC, Ghosh S, Roy SK (2012) *J Mol Struct* 1027:36–43
- Pal K, Majumder TP, Schirhagl R, Ghosh S, Roy SK, Dabrowski R (2013) *Appl Surf Sci* 280:405–417
- Pal K, Mohan MLNM, Zhan B, Wang G (2015) *J Mater Chem C* 3:11907
- Pal K, Zhan B, Wang G, Mohan MLNM, Schirhagl R (2015) *Appl Surf Sci* 357:1499–1510
- Saravanan S, Silambarasan M, Soga T (2014) *J Appl Phys* 53:1–6
- Mohan R, Ravichandran K, Nithya A, Jothivenkatachalam K, Ravidhas C, Sakthivel B (2014) *Mater Sci: Mater Electron* 25:2546–2553
- Gayathri S, Nirmal Ghosh OS, Sathishkumar S, Sudhakara P, Jayaramudu J, Ray SS, Kasi Viswananath A (2015) *Appl Sci Lett* 1:8–13
- Bandyopadhyay S, Paul CK, Roy R, Sen SK, Sen S (2002) *Mater Chem Phys* 74:83–91
- Labhane PK, Huse VR, Patle LB, Chaudhari AL, Sonawane GH (2015) *J Mater Sci Chem Eng* 3:39–51
- Thakur S, Sharma N, Varkia A, Kumar J (2014) *Adv Appl Sci Res* 5:18–24
- Ravichandran K, Saravanakumar K, Chandramohan R, Nandhakumar V (2012) *Appl Surf Sci* 261:405–410
- Patterson AL (1939) *Phys Rev* 56:978
- Cao H, Zhao YG, Ong HC, Ho ST, Dai JY, Wu JY, Chang RPH (1998) *Appl Phys Lett* 73:3656–3658
- Kwon YJ, Kim KH, Lim CS (2002) *J Ceram Proc Res* 3:146–149
- Silva RF, Zaniquelli MED (2002) *Colloid Surf Physicochem Eng Aspect* 198:551–558
- Murtaza G, Ahmad R, Rashid M, Hassan M, Hussain A, Khan MA, Ehsan ul Haq M, Shafique M, Riaz S (2014) *Curr Appl Phys* 14:176–181
- Ram M, Arya GS, Parmar K, Kotnala RK, Negi NS (2015) *Int J Adv Eng Technol* 8:329–336
- Hosseini SM, Abdolhosseini Sarsari I, Kameli P, Salamati H (2015) Effect of Ag doping on structural, optical, and photocatalytic properties of ZnO nanoparticles. *J Alloys Compd* 640:408–415
- Ravichandran K, Anbazhagan A, Beneto M, Dineshbabu N, Ravidhas C (2016) *Mater Sci Semicond Process* 41:150–154
- Menon AS, Kalarikkal N, Thomas S (2013) *Ind J Nano Sci* 1:16–24
- Ravichandran K, Rathi R, Beneto M, Karthika K, Rajkumar PV, Sakthivel B, Damodaran R (2015) *Ceram Int* 41:3390–3395
- Sagadevan S, Das I, Poddar J (2016) *J Mater Sci: Mater Electron* 27:13016–13021
- Prabaharan DMDM, Sadaiyandi K, Mahendran M, Sagadevan S (2016) *Mater Res* 19:478–482

34. Sagadevan S, Das I, Singh P, Poddar J (2017) *J Mater Sci: Mater Electron* 28:1136–1141
35. Roy AK, Singh A, Kumari K, Amar Nath K, Prasad A, Prasad K (2012) *ISRN Ceramics* 2012:1–10
36. Funke K (1993) *Prog Solid State Chem* 22(2):111–195
37. Almond DP, Bowen CR (2004) *Phys Rev Lett* 92(15):5
38. Bowen CR, Almond DP (2006) *Mater Sci Technol* 22:719–724
39. Sagadevan S, Pal K (2017) *J Mater Sci: Mater El* doi:[10.1007/s10854-017-6640-0](https://doi.org/10.1007/s10854-017-6640-0)
40. Sagadevan S, das I, Pal K, Murugasen P, Singh P (2016) *J Mater Sci: Mater Electron* 28:1–9. doi:[10.1007/s10854-016-6180-z](https://doi.org/10.1007/s10854-016-6180-z)